Numerical studies of phase for the angular Talot effect

Khebbache N., Djabi S. and Ferria K.

Laboratory of Photonic Systems and Nonlinear Optics, Institute of Optics and Fine Mechanics, University of Setif 1, 19000 Algeria,
e-mail: khebbachenaima@univ-setif.dz

Abstract. We provide a numerical study of phase observed at the angular Talbot effect for both one- and two-dimensional gratings. The effect allows for fractional self-imaging in the vicinity of the grating which is illuminated by the wave with a spherical front at different Talbot distances.

1. Introduction

The effect of self-imaging has been observed in 1836 by H. F. Talbot. Its explanation is based on the theory of scalar diffraction. The diffracted field is seen as superposition of replicas translated and weighted by the initial field; the number of the replicas is only linked to the fractional order (a so-called fractional Talbot effect). Rayleigh has successfully explained this phenomenon as interference of the diffracted beams in the paraxial approximation [1, 2].

The Talbot effect has opened the door for many applications such as laser sources [3], optical communications [4], plasmonics [5], matter–wave interactions [6], quantum mechanics [7], imagery [8], and medicine [9]. Many researchers have analyzed a self-imaging observed in the near field (i.e., in the Fresnel approximation), while the other have focused on the diffraction intensity distribution [10, 11] and how to simplify computation of the Fresnel transformation [12].

Notice that, in all of the studies mentioned above, the results for the Talbot effect have been examined for the case of the near field. Nonetheless, a recent work [13] has proved that the Talbot effect can also be generated in the far field, thus giving rise to a new phenomenon which has been termed as the 'angular Talbot effect'.

Following this approach, below we report on numerical studies of the angular Talbot effect observed under illumination of the grating with a parabolic wave front. Our analysis is associated with the phase observed at the angular Talbot effect, which is directly derived from the far-field approximation employed for the cases of one- and two-dimensional grating. As in Ref. [13], we study theoretically the angular Talbot effect for the case of 1D grating, and then extend the theory for describing 2D gratings.

2. Theoretical aspects of the phase observed at the angular Talbot effect

Assume that an amplitude diffraction grating (the aperture Λ) is illuminated by a wave with spherical front and the wavelength λ (see Fig. 1). The grating is located at the distance $d = pZ_t / q$ from a source S1, where p and q are coprime integers and Z_t denotes the distance at which the periodic wave front is fully reproduced. It is called a Talbot distance and is expressed as $Z_t = \Lambda^2 / \lambda$.
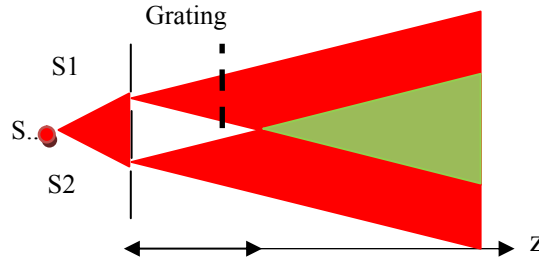
Fig. 1. Illustration of phase observed at the angular Talbot effect using interference of two spherical waves. A grating is illuminated by a spherical wave generated by a source S1 located at a distance *d*. Green zone describes interference of the diffracted orders with the wave generated by another source S2.

2.1. 1D grating

The transmission function of a 1D grating is given by

$$t(x) = g(x) \otimes \left[t_{env}(x) \sum_{n=-\infty}^{+\infty} \delta(x - n\Lambda) \right], \qquad (1)$$

where $g(x)$ is the complex transmission function that varies over the elementary grating aperture and $t_{env}(x)$ the transmission function varying over the slits of the grating (their role being to collect all the diffraction orders – see Ref. [14]). The transmission function can be convoluted by a train of Dirac deltas (comb functions) $\delta(x - n\Lambda)$ located at the positions $n\Lambda$ and spaced by the intervals Λ:

$$FT\left[t(x)\right] = \tilde{t}(k_x) = \tilde{g}(k_x) \sum_{n=-\infty}^{+\infty} t_{env}(n\Lambda) \exp(i\Lambda n k_x). \qquad (2)$$

Here $FT\left[g(x)\right] = \tilde{g}(k_x)$ is the Fourier transform and *x* the spatial coordinate. Then the spatial frequency k_x becomes a transform variable. The electric field observed for the case of a parabolic wave can be written as

$$E(x) \propto \exp\left(i\frac{\pi}{\lambda d} x^2 \right) g(x) \otimes \left(t_{env}(x) \sum_{n=-\infty}^{+\infty} \delta(x - n\Lambda) \right). \qquad (3)$$

The exponential term involved in Eq. (3) indicates a quadratic phase curvature. The Fourier transform of the electric field at the location $n\Lambda$ is given by

$$\tilde{E}(x) \propto G(k_x) \sum_{n=-\infty}^{+\infty} t_{env}(n\Lambda) \exp(ink_x\lambda) \exp\left(-i\frac{\pi n^2 \Lambda^2}{\lambda d} \right). \qquad (4)$$

After substituting the term Λ^2 / λ Eq. (4) becomes as follows:

$$\tilde{E}(x) \propto G(k_x) \sum_{n=-\infty}^{+\infty} t_{env}(n\Lambda) \exp(ink_x\lambda) \exp\left(-i\frac{\pi n^2 Z t}{d} \right), \qquad (5)$$

or

$$\tilde{E}(x) \propto G(k_x) \sum_{n=-\infty}^{+\infty} t_{env}(n\Lambda) \exp(ink_x\lambda) \exp\left(-i\frac{\pi n^2 q}{p} \right). \qquad (6)$$

The second exponential term in Eq. (6) indicates that the quadratic phase depends on the coprime integers p and q.

2.2. 2D grating

To represent the field diffracted by a 2D grating in the far field, we follow the same steps as in the 1D case. However, now we should add the spatial coordinate y and the spatial frequency k_y. Then the transmission function of the 2D grating can be expressed in the form

$$t(x,y) = g(x,y) \otimes \left[t_{env}(x,y) \sum_{n=-\infty}^{+\infty} \sum_{m=-\infty}^{+\infty} \delta(x-n\Lambda, y-m\Lambda) \right],$$ (7)

where $\otimes$ denotes the convolution operation, $g(x,y)$ the complex transmission function that varies over the elementary grating aperture, $t_{env}(x,y)$ the transmission function varying over the slits of the 2D grating, and $\delta(x-n\Lambda, y-m\Lambda)$ is again the train of the Dirac deltas spaced at the intervals Λ and located at the positions $n\Lambda$ and $m\Lambda$ respectively along the x and y directions. The Fourier transform of $t(x,y)$ is as follows:

$$\tilde{t}(k_x, k_y) = \tilde{g}(k_x, k_y) \sum_{n=-\infty}^{+\infty} \sum_{m=-\infty}^{+\infty} t_{env}(n\Lambda, m\Lambda) \exp[i\Lambda(nk_x + mk_y)],$$ (8)

where $\tilde{g}(k_x, k_y)$ implies the Fourier transform of $g(x,y)$.

The electric field for the case of parabolic wave is given by

$$E(x,y) \propto \exp\left(i\frac{\pi}{\lambda d}(x^2 + y^2) \right) g(x,y) \otimes \left(t_{env}(x,y) \sum_{n=-\infty}^{+\infty} \sum_{m=-\infty}^{+\infty} \delta(x-n\Lambda, y-m\Lambda) \right),$$ (9)

whereas its Fourier transforms can be written as

$$\tilde{E}(x,y) \propto G(k_x, k_y) \sum_{n=-\infty}^{+\infty} \sum_{m=-\infty}^{+\infty} t_{env}(n\Lambda, m\Lambda) \exp\left(i(nk_x + mk_y)\Lambda \right) \times \exp\left(-i\frac{\pi}{\lambda} \frac{(n^2 + m^2)\Lambda^2}{d} \right).$$ (10)

The second exponential term in Eq. (10) again indicates the quadratic phase (see Ref. [15]) that depends on the coprime integers p and q.

3. Results and discussion

As already mentioned, the Talbot effect appears when the diffracted orders interfere with each other and disappears when they get separated. More precisely, the effect depends on the phase of the diffracted orders. If the latter are in phase we observe the image of the grating, otherwise the angular Talbot effect pattern is generated (i.e., the diffracted orders have a quadratic phase).

Assume that the 1D grating is made of N slits and the 2D grating of $N*N$ slits. We have used numerical simulations with Matlab to derive the phase observed at the angular Talbot effect under the conditions of different Talbot distances. The main results are displayed in Fig. 2 and Fig. 3.

The term $\exp(i\pi x^2/\lambda d)$ in Eq. (3) is responsible for the parabolic shape of the phase pattern displayed in Fig. 2a for the 1D gratings. Besides, for many p/q ratios one can see that the periodic patterns remain the same when we change the integer p and keep q constant. This is contrary to the case when p is kept constant and q changed, which leads to changing periodic patterns. In this relation we remind that the variation of the phase observed at the angular Talbot effect depends on q.
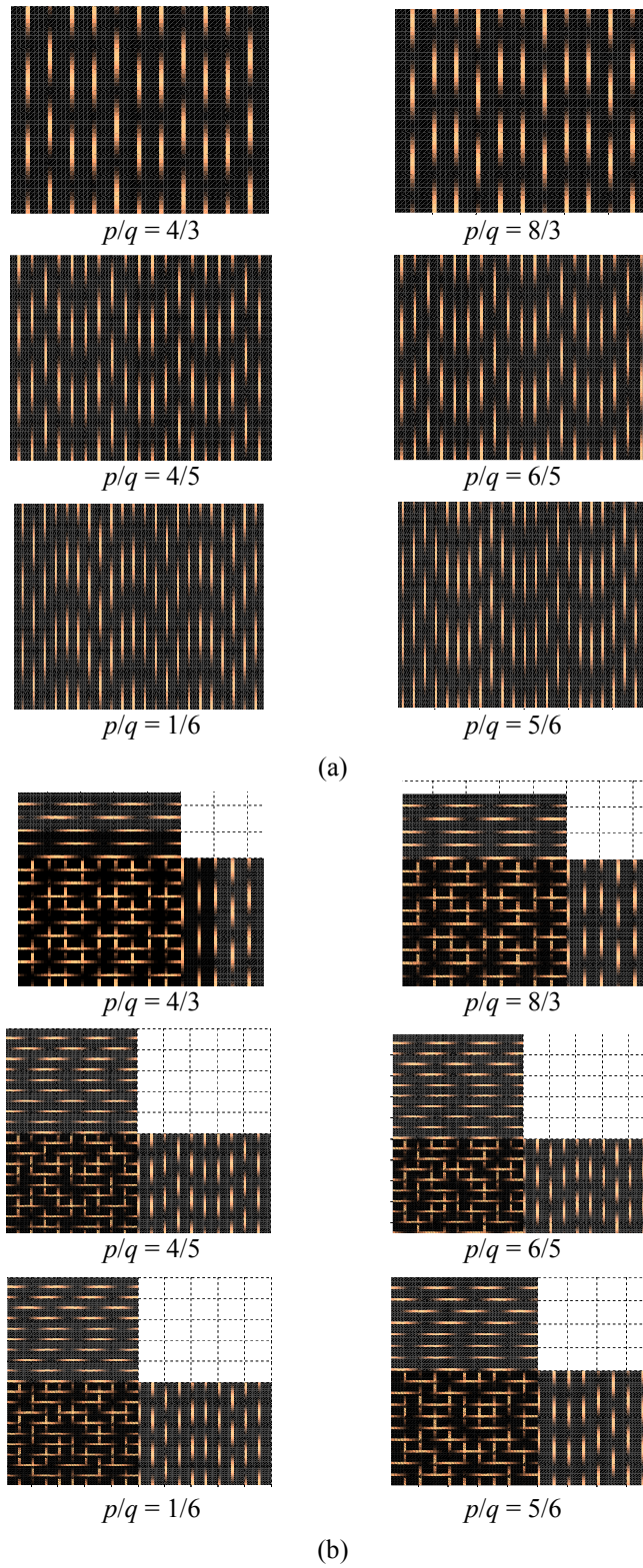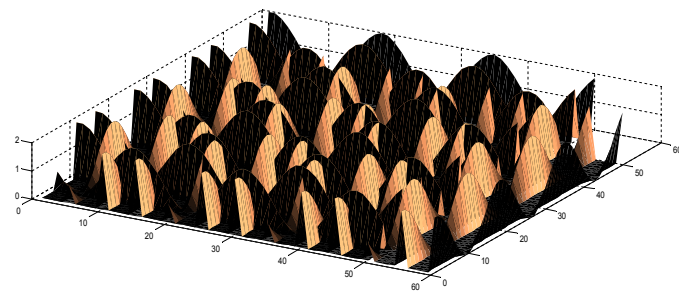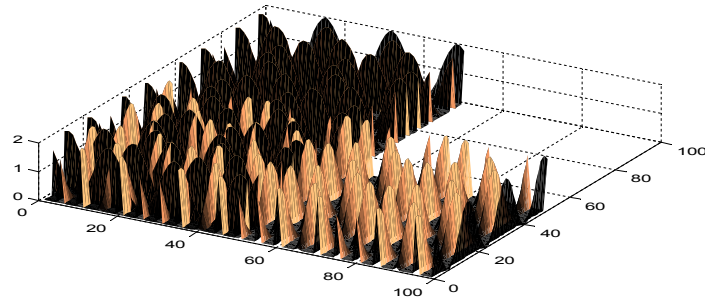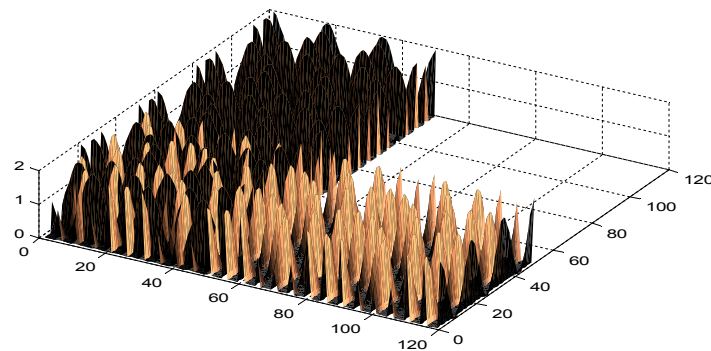
p/q = 4/3   *p/q* = 8/3

p/q = 4/5   *p/q* = 6/5

p/q = 1/6   *p/q* = 5/6

(a)

p/q = 4/3   *p/q* = 8/3

p/q = 4/5   *p/q* = 6/5

p/q = 1/6   *p/q* = 5/6

(b)

Fig. 2. Phase patterns simulated for 1D (a) and 2D (b) gratings at different *p/q* ratios. Right and upper images in panel (b) describe the phase patterns observed in the cases of constituent 1D gratings arranged along the *y* and *x* directions, respectively.

$p/q = 4/3$

$p/q = 4/5$

$p/q = 5/6$

Fig. 3. 3D representations of the phase simulated at the Talbot effect for different *p/q* ratios. Copper and black colours correspond to the phase patterns observed for the constituent 1D gratings arranged respectively along the *x* and *y* directions, and mixed colour to the case when the two gratings are superimposed.

The term $\exp[i\pi(x^2 + y^2)/\lambda d]$ present in Eq. (9) proves that the parabolic shape can also be observed in the case of 2D gratings. Our idea has been to consider the 2D grating as a superposition of two mutually perpendicular 1D gratings of the same size and the same slits number. However the patterns shown in Fig. 2b for the case when two 1D gratings are intersected reveal an unclear parabolic shape (cf. with Fig. 2a). A clearer manifestation of the parabolic shape for the 2D gratings comes from the simulations performed in 3D space (see Fig. 3).

In addition to testifying a clear parabolic shape explained by the term $\exp[i\pi(x^2 + y^2)/\lambda d]$, Fig. 3 also demonstrates that the number of replicas and the distance *d* between the source and the grating are interconnected. The latter decreases with increasing number of replicas, according to the relationship $d = p/q Z_t$. Therefore the distance *d* is evidently proportional to the integer *p*. Eqs. (6) and (10) simply demonstrate that the quadratic terms $\exp(-i\pi n^2 q/p)$ and $\exp(i\pi(n^2 + m^2)q/p)$ are proportional to *q*. Then the number of replicas depends directly on the increase in the *q* parameter.

4. Conclusion

In this work we have suggested a new approach to analyzing the phase observed at the angular Talbot effect, which is based on the Fraunhofer diffraction. In fact this new class of the Talbot effects, the angular Talbot effect, can be considered as an extremely simplified version, for which the analytical analysis of the phase is less complicated when compared with the near–field case. Our simulation results for the both 1D and 2D gratings testify a parabolic-shaped phase depending on the exponential terms involved respectively in Eqs. (3) and (9). We have also demonstrated that the period of the phase depends on the integer q and the replicas number increases with its increasing. We believe that the effects for the phase observed at the angular Talbot effect can facilitate new applications in the time, spatial and spectral domains.

References

1. Talbot H F, 1836. Facts relating to optical science. Phil. Mag. **9**: 401–407.
2. Rayleigh L, 1881. On copying diffraction gratings, and some phenomena connected therewith. Phil. Mag. **11**: 196–205.
3. Guillet de Chatellus H, Lacot E, Glastre W, Jacquin O, Hugon O and Marklof J, 2013. Generation of ultrahigh and tunable repetition rates in CW injection-seeded frequency-shifted feedback lasers. Opt. Expr. **21**: 15065–15074.
4. Jeremy A. Bolger, Peifang Hu, Joe T, Mok J L, Justin L. Blows and Benjamin Eggleton, 2005. Talbot self-imaging and cross-phase modulation for generation of tunable high repetition rate pulse trains. Opt. Commun. **249**: 431–439.
5. Weiwei Z, Chenlong Z, Jiayuan W and Jiasen Z, 2009. An experimental study of the plasmonic Talbot effect. Opt. Expr. **17**: 19757–19762.
6. Yiting Y, Delphine C, Torsten S, Benjamin L and Hans Z, 2013. The focusing and Talbot effect of periodic arrays of metallic nanoapertures in high-index medium. Plasmonics, **8**: 723–732.
7. Berry M, Marzoli I and Schleich W, 2001. Quantum carpets. Phys. World. 14: 1439–1444.
8. Wang A, Gill P and Molnar A, 2009. Light field image sensors based on the Talbot effect. Appl. Opt. **48**: 5897–5905.
9. Ryotaro S, Takashi S, Kazuhiko U, Shinichi K, Masayuki H, Toshifumi M, Naoki N and Yoko H, 2006. Measurement of wavefront aberration of human eye using Talbot image of two-dimensional grating. Opt. Rev. **13**: 207–211.
10. Berry M V and Klein S, 1996. Integer, fractional and fractal Talbot effects. J. Mod. Opt. **43**: 2139–2164.
11. Shuyun T, Tongjun Z and Chuanfu C, 2008. Influence of the size of the grating on Talbot effect. Optik. **119**: 695–699.
12. De Bougrenet J L, De La Tocnaye and Hamam H, 1995. The fractional Fresnel transform. J.Optics, **26**: 49–56.
13. Azaña J and Guillet de Chatellus H, 2014. Angular Talbot effect. Phys. Rev. Lett. **112:** 213902.
14. Del Mar Sánchez-López M, Moreno I and Martínez-García A, 2009. Teaching diffraction gratings by means of a phasor analysis. Proc. of ETOP Conference, 1–12.
15. Goodman J E. Introduction to Fourier optics, 2nd Ed. (New York: McGraw-Hill, 1996).

Анотація. *У роботі представлено результати досліджень фази світлової хвилі на основі числового моделювання кутового ефекту Талбота для одно- і двовимірної граток. Ефект дає змогу спостерігати дробове самовідтворення зображення біля гратки, опроміненої сферичними хвилями за умови різних відстаней Талбота.*